Market-based Coordination of Integrated Electricity & Natural Gas Systems Under Uncertain Supply

Christos Ordoudis, Stefanos Delikaraoglou, Jalal Kazempour, Pierre Pinson

This document serves as an electronic companion (EC) for the paper "Market-based Coordination of Integrated Electricity and Natural Gas Systems under Uncertain Supply". It contains four sections that present the MPEC formulation of the bilevel model *V-B*, a schematic representation of the supply curve for *Seq*, *Stoch*, *V-B* and *P-B* dispatch models, a schematic representation of one pipeline and the variables in relation to the approximation of the natural gas flow and additional results.

1. MPEC formulation of volume-based coupled electricity and natural gas model (V-B)

In this section the bilevel *V-B* model is reformulated as a Mathematical Program with Equilibrium Constraints (MPEC) by replacing the linear, and thus convex, lower level problems by their Karush-Kuhn-Tucker (KKT) conditions. Then, the resulting MPEC is transformed into a Mixed-Integer Linear Program (MILP) in order to deal with the bilinear terms that arise from the complementarity conditions. We introduce a mapping $M_a^{i_g}$ of the natural gas-fired power plants i_g at area a (entries are equal to 1 if a GFPP is connected to an area and 0 otherwise). The model writes as follows,

$$\underset{\Theta^{\text{MUL}}}{\text{Min.}} \sum_{t\in T}\Big[\sum_{i_c\in I_c} C_{i_c}p_{i_c,t} + \sum_{k\in K} C_k g_{k,t} + \sum_{\omega\in\Omega}\pi_\omega\Big(\sum_{k\in K}(C_k^+ g^+_{k,\omega,t} - C_k^- g^-_{k,\omega,t}) + \sum_{i_c\in I_c}(C^+_{i_c}p^+_{i_c,\omega,t} - C^-_{i_c}p^-_{i_c,\omega,t}) + \sum_{r_e\in R_e} C^{\text{sh,E}} l^{\text{sh,E}}_{r_e,\omega,t} + \sum_{r_g\in R_g} C^{\text{sh,G}} l^{\text{sh,G}}_{r_g,\omega,t}\Big)\Big] \tag{1a}$$

$$\text{s.t } -p_{i,t} \le \Delta p_{i,\omega',t} \le P_i^{\max} - p_{i,t},\ \ \forall i,t, \tag{1b}$$

$$-P_i^- \le \Delta p_{i,\omega',t} \le P_i^+,\ \ \forall i,t, \tag{1c}$$

$$0 \le w^{\text{sp}}_{j,\omega',t} \le W_{j,\omega',t},\ \ \forall j,t, \tag{1d}$$

$$0 \le l^{\text{sh,E}}_{r_e,\omega',t} \le D^{\text{E}}_{r_e,t},\ \ \forall t, \tag{1e}$$

$$\sum_{i\in I}\Delta p_{i,\omega',t} + \sum_{r_e\in R_e} l^{\text{sh,E}}_{r_e,\omega',t} + \sum_{j\in J}(W_{j,\omega',t} - w^{\text{sp}}_{j,\omega',t} - w_{j,t}) = 0 : \tilde{\lambda}^{\text{E}}_{\omega',t},\ \ \forall t, \tag{1f}$$

$$-g_{k,t} \le \Delta g_{k,\omega',t} \le G_k^{\max} - g_{k,t},\ \ \forall k,t, \tag{1g}$$

$$-G_k^- \le \Delta g_{k,\omega',t} \le G_k^+,\ \ \forall k,t, \tag{1h}$$

$$0 \le l^{\text{sh,G}}_{r_g,\omega',t} \le D^{\text{G}}_{r_g,t},\ \ \forall t, \tag{1i}$$

$$\sum_{k\in K}\Delta g_{k,\omega',t} + \sum_{r_g\in R_g} l^{\text{sh,G}}_{r_g,\omega',t} - \sum_{i_g\in I_g}\phi_{i_g}\Delta p_{i_g,\omega',t} = 0 : \tilde{\lambda}^{\text{G}}_{\omega',t},\ \ \forall t, \tag{1j}$$

$$0 \le \sum_{t\in T}\sum_{i_g\in A_z^{I_g}}\phi_{i_g}(p_{i_g,t} + \Delta p_{i_g,\omega',t}) \le F_z^{\text{A}},\ \ \forall z, \tag{1k}$$

$$0 \le \sum_{i_g\in A_z^{I_g}}\phi_{i_g}(p_{i_g,t} + \Delta p_{i_g,\omega',t}) \le F^{\text{M}}_{z,t},\ \ \forall z,t, \tag{1l}$$

$$0 \le \chi^v_\psi \le |T|\sum_{k\in K} G_k^{\max} - \sum_{t\in T}\sum_{r_g\in R_g} D^{\text{G}}_{r_g,t},\ \ \forall \psi, \tag{1m}$$

$$0 \leq \chi^{v}_{\psi,t} \leq F^{\max}_{\psi,t} - \sum_{r_g \in A^{R_g}_{\psi}} D^{\mathrm{G}}_{r_g,t}, \ \ \forall \psi, t, \tag{1n}$$

$$0 \leq p_{i,t} \leq P^{\max}_{i} : \underline{\mu}^{\mathrm{P}}_{i,t}, \overline{\mu}^{\mathrm{P}}_{i,t}, \ \ \forall i, t, \tag{1o}$$

$$0 \leq w_{j,t} \leq \widehat{W}_{j,t} : \underline{\mu}^{\widehat{\mathrm{W}}}_{j,t}, \overline{\mu}^{\widehat{\mathrm{W}}}_{j,t}, \ \ \forall j, t, \tag{1p}$$

$$\sum_{i \in I} p_{i,t} + \sum_{j \in J} w_{j,t} - \sum_{r_e \in R_e} D^{\mathrm{E}}_{r_e,t} = 0 : \hat{\lambda}^{\mathrm{E}}_{t}, \ \ \forall t, \tag{1q}$$

$$0 \leq g_{k,t} \leq G^{\max}_{k} : \underline{\mu}^{\mathrm{G}}_{k,t}, \overline{\mu}^{\mathrm{G}}_{k,t}, \ \ \forall k, t, \tag{1r}$$

$$\sum_{k \in K} g_{k,t} - \sum_{r_g \in R_g} D^{\mathrm{G}}_{r_g,t} - \sum_{i_g \in I_g} \phi_{i_g} p_{i_g,t} = 0 : \hat{\lambda}^{\mathrm{G}}_{t}, \ \ \forall t, \tag{1s}$$

$$0 \leq \sum_{t \in T} \sum_{i_g \in A^{I_g}_{\psi}} \phi_{i_g} p_{i_g,t} \leq x^{v}_{\psi} : \underline{\nu}^{v}_{\psi}, \overline{\nu}^{v}_{\psi}, \ \ \forall \psi, \tag{1t}$$

$$0 \leq \sum_{i_g \in A^{I_g}_{\psi}} \phi_{i_g} p_{i_g,t} \leq x^{v}_{\psi,t} : \underline{\mu}^{v}_{\psi,t}, \overline{\mu}^{v}_{\psi,t}, \ \ \forall \psi, t \tag{1u}$$

$$C_{i_c} - \hat{\lambda}^{\mathrm{E}}_{t} - \underline{\mu}^{\mathrm{P}}_{i_c,t} + \overline{\mu}^{\mathrm{P}}_{i_c,t} = 0, \ \ \forall i_c, t, \tag{1v}$$

$$\phi_{i_g} \hat{\lambda}^{\mathrm{G}}_{t} - \hat{\lambda}^{\mathrm{E}}_{t} - \underline{\mu}^{\mathrm{P}}_{i_g,t} + \overline{\mu}^{\mathrm{P}}_{i_g,t} + \sum_{\psi \in \Psi} M^{i_g}_{\psi} (\phi_{i_g} \overline{\mu}^{v}_{\psi,t} + \phi_{i_g} \overline{\nu}^{v}_{\psi} - \phi_{i_g} \underline{\mu}^{v}_{\psi,t} - \phi_{i_g} \underline{\nu}^{v}_{\psi}) = 0, \ \ \forall i_g, t, \tag{1w}$$

$$- \hat{\lambda}^{\mathrm{E}}_{t} - \underline{\mu}^{\widehat{\mathrm{W}}}_{j,t} + \overline{\mu}^{\widehat{\mathrm{W}}}_{j,t} = 0, \ \ \forall j, t, \tag{1x}$$

$$C_{k} - \hat{\lambda}^{\mathrm{G}}_{t} - \underline{\mu}^{\mathrm{G}}_{k,t} + \overline{\mu}^{\mathrm{G}}_{k,t} = 0, \ \ \forall k, t, \tag{1y}$$

$$0 \leq \overline{\mu}^{\mathrm{P}}_{i,t} \perp P^{\max}_{i} - p_{i,t} \geq 0, \ \ \forall i, t, \tag{1z}$$

$$0 \leq \underline{\mu}^{\mathrm{P}}_{i,t} \perp p_{i,t} \geq 0, \ \ \forall i, t, \tag{1aa}$$

$$0 \leq \overline{\mu}^{\widehat{\mathrm{W}}}_{j,t} \perp \widehat{W}_{j} - w_{j,t} \geq 0, \ \ \forall j, t, \tag{1ab}$$

$$0 \leq \underline{\mu}^{\widehat{\mathrm{W}}}_{j,t} \perp w_{j,t} \geq 0, \ \ \forall j, t, \tag{1ac}$$

$$0 \leq \overline{\mu}^{v}_{\psi,t} \perp x^{v}_{\psi,t} - \sum_{i_g \in A^{I_g}_{\psi}} \phi_{i_g} p_{i_g,t} \geq 0, \ \ \forall \psi, t, \tag{1ad}$$

$$0 \leq \overline{\nu}^{v}_{\psi} \perp x^{v}_{\psi} - \sum_{t \in T} \sum_{i_g \in A^{I_g}_{\psi}} \phi_{i_g} p_{i_g,t} \geq 0, \ \ \forall \psi, \tag{1ae}$$

$$0 \leq \underline{\mu}^{v}_{\psi,t} \perp \sum_{i_g \in A^{I_g}_{\psi}} \phi_{i_g} p_{i_g,t} \geq 0, \ \ \forall \psi, t, \tag{1af}$$

$$0 \leq \underline{\nu}^{v}_{\psi} \perp \sum_{t \in T} \sum_{i_g \in A^{I_g}_{\psi}} \phi_{i_g} p_{i_g,t} \geq 0, \ \ \forall \psi, \tag{1ag}$$

$$0 \leq \overline{\mu}^{\mathrm{G}}_{k,t} \perp G^{\max}_{k} - g_{k,t} \geq 0, \ \ \forall k, t, \tag{1ah}$$

$$0 \leq \underline{\mu}^{\mathrm{G}}_{k,t} \perp g_{k,t} \geq 0, \ \ \forall k, t, \tag{1ai}$$

The nonlinearities that arise from complementarity conditions are linearized via the Fortuny-Amat transformation [1]. We introduce the set of dual variables (λ, μ and ν) Θ^{dual}, thus $\Theta^{\mathrm{MUL}} = \{\Theta^{\mathrm{VUL}}, \Theta^{\mathrm{VLL}}, \Theta^{\mathrm{dual}}\}$. For the network constrained balancing market, we use the set of constraints {(2b)-(2e),(2g)-(2i),(3a)-(3c),(6a)-(6p)} (numbered from the original manuscript) instead of (1b)-(1l).

2. Schematic representation of the supply curve

The day-ahead scheduling that can be obtained by the four different dispatch models, *Seq*, *Stoch*, *V-B* and *P-B*, is illustrated in Figures 1-5. More specifically, the supply curve is presented in a simple setup with one stochastic producer, two non-GFPPs and two GFPPs for a single time period. The aim is to illustrate the way that the volume-based and price-based models affect the position of the power plants at the supply curve and approximate the stochastic dispatch solution. The following analysis and Figures 1-5 come from [2].

Figures 1 and 2 present the merit-order curve under the sequential dispatch and the stochastic dispatch models. The stochastic producer (e.g. wind power) is dispatched first due to the very low or zero marginal cost. It can be observed the power plants are scheduled based on an ascending order of marginal costs (i.e. merit-order principle) until the demand is covered in the sequential model. On the other hand, the stochastic dispatch model may schedule some power plants out of merit order. This decision depends on the structure of scenario set Ω that is available at the day-ahead stage. The power plants are scheduled in a way that cost-effective capacity is revealed for the real-time operation. However, the resulting prices guarantee cost recovery for flexible producers and revenue adequacy for the system/market operator only in expectation [3].

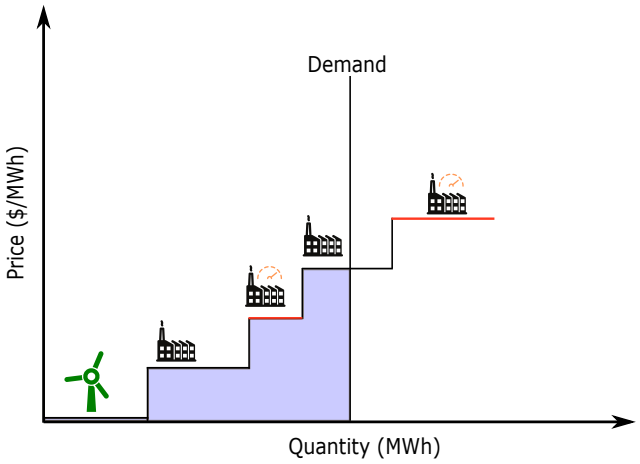

Figure 1. Supply curve when scheduling the day-ahead stage via the sequential dispatch model, where GFPPs are indicated with the red line (Figure from [2]).

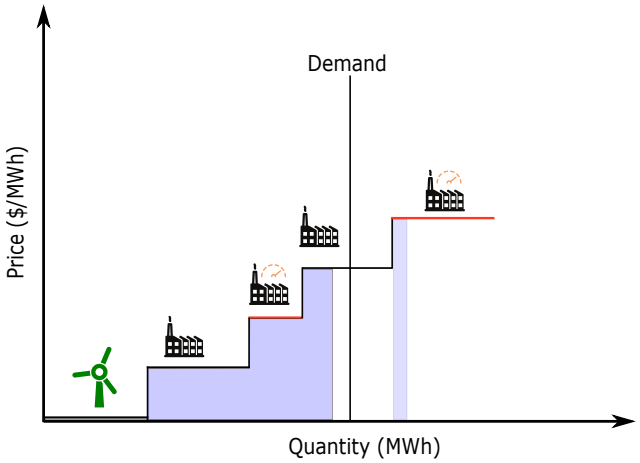

Figure 2. Supply curve when scheduling the day-ahead stage via the stochastic dispatch model, where GFPPs are indicated with the red line (Figure from [2]).

The effect of χ^v, which is defined by two variants of the volume-based dispatch model, on the merit order is depicted in Figures 3 and 4. When natural gas volume availability χ^v is defined for the whole natural gas system, a decrease of χ^v affects the most expensive GFPP. In this example, it can be noticed that the single GFPP is scheduled less and the marginal power producer is scheduled more by still respecting the merit-order principle. Defining χ^v individually for each GFPP permits to alter the schedule of both GFPPs by decreasing the volume made available for the cheap GFPP and in turn increasing the availability for the expensive GFPP. In both cases, the volume-based models are able to reveal cost-effective flexibility for balancing but simultaneously follow the merit-order principle that guarantees cost recovery for each scenario in Ω.

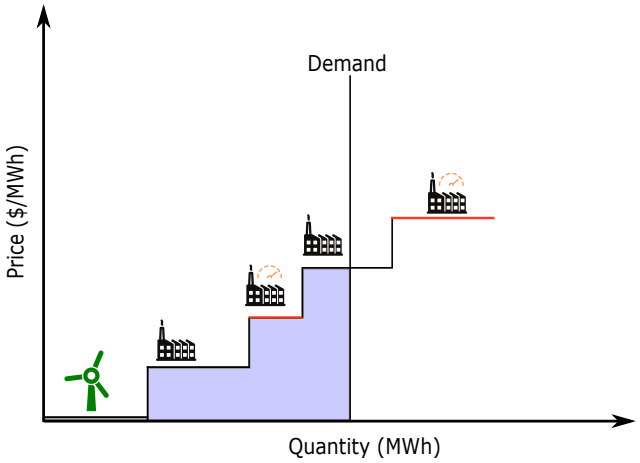

FIGURE 3. Supply curve when scheduling the day-ahead stage via the volume-based dispatch model, where GFPPs are indicated with the red line (Figure from [2]).

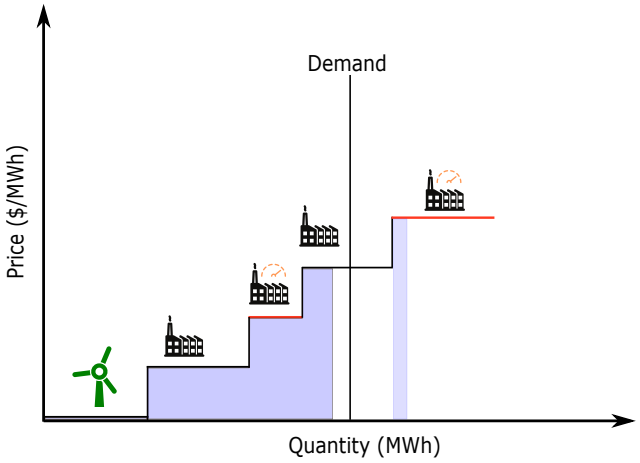

FIGURE 4. Supply curve when scheduling the day-ahead stage via the stochastic dispatch model, where GFPPs are indicated with the red line (Figure from [2]).

A similar effect is noticed in Figure 5, where the solution of the stochastic model is approximated by the price-based dispatch model that schedules the power plants based on the ascending order of marginal costs. In this case, the system/market operator decreases the natural gas price perceived by GFPPs which results in decreasing their marginal cost and scheduling the most expensive GFPP. Note that natural gas price adjustment is the same for all GFPPs; we illustrate though the effect only for the most expensive GFPP for clarity. A similar outcome may be accomplished by increasing the natural gas perceived by GFPPs. In this case, the schedule of the cheap GFPP would be affected.

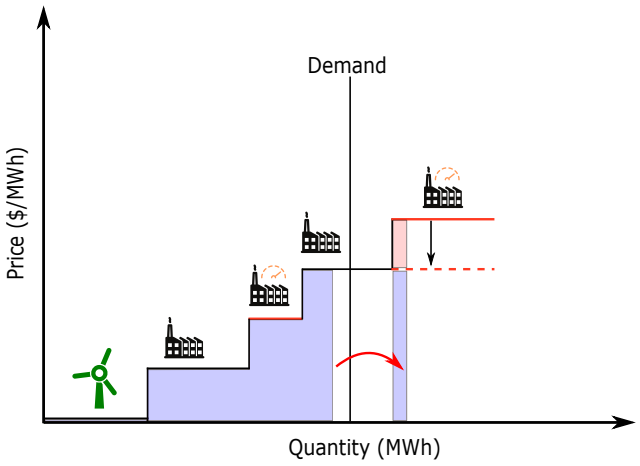

FIGURE 5. Supply curve when scheduling the day-ahead stage via the price-based dispatch model, where GFPPs are indicated with the red line (Figure from [2]).

3. Schematic representation of pipeline

A schematic representation of one pipeline and the variables in relation to the approximation of the natural gas flow is presented in Figure 6. Figure 6 serves as a supplement to equations (4)-(7) of the original manuscript.

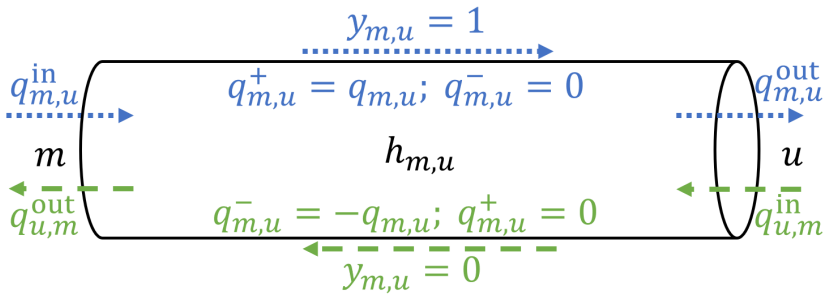

Figure 6. Bidirectional flow along a pipeline (Figure from [4])

4. Additional Results

Fig. 7 shows the natural gas price adjustment (χ_t^p) and the day-ahead payment/charge in order to generate this signal. Moreover, Fig. 8 illustrate the natural gas price adjustment (χ_t^p) in relation to the difference in the hourly GFPPs' share of the total power production between *P-B* and *Seq*. A detailed analysis of these results is presented in [5].

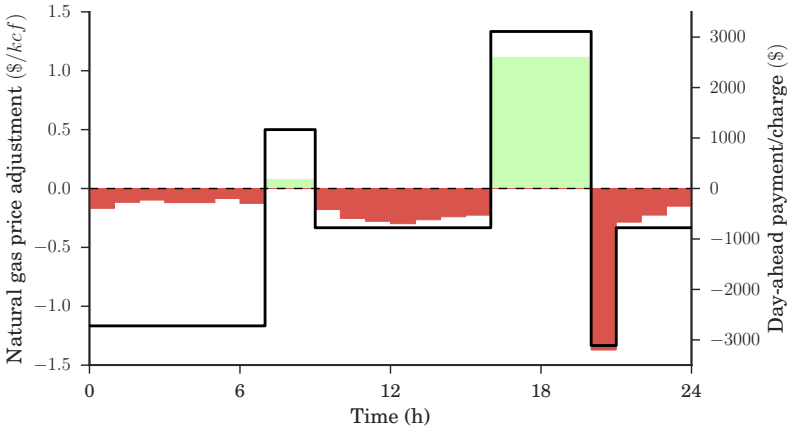

Figure 7. Hourly natural gas price adjustment (black line: left y-axis) and day-ahead financial settlement of the system operator to adjust the natural gas price (colored areas: right y-axis). Wind power penetration 50%. (Figure from [5])

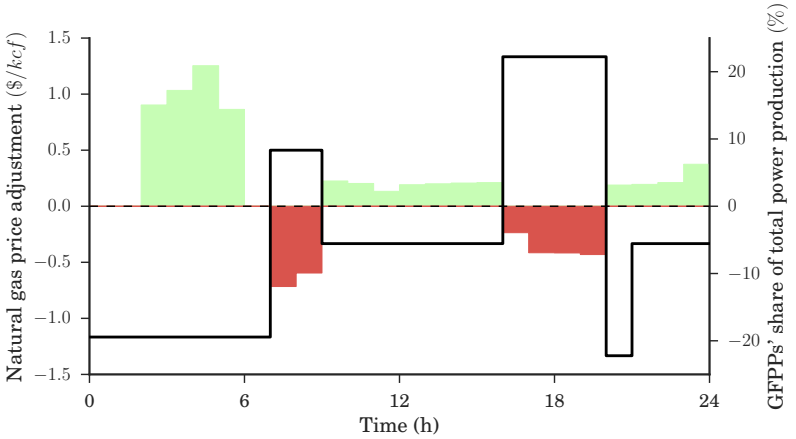

Figure 8. Hourly natural gas price adjustment (black line: left y-axis) and difference in GFPPs' share of total power production between P-B and Seq (colored areas: right y-axis). Wind power penetration 50%. (Figure from [5])

Figue 9 shows the natural gas volume ($\chi^v_{a,t}$) in relation to the natural gas volume consumed in *Seq* and the the difference in the hourly GFPPs' share of the total power production between *V-B* and *Seq*. Moreover, Figure 10 illustrate the natural gas volume ($\chi^v_{a,t}$) change compared to the natural gas volume consumed in *Seq* in relation to the difference in the hourly GFPPs' share of the total power production between *V-B gen* and *Seq*. Thus, the left y-axis illustrates the quantity $\frac{F(V\text{-}B)-F(Seq)}{F(Seq)}$ or $\frac{F(V\text{-}B\ gen)-F(Seq)}{F(Seq)}$, where F is the natural gas volume made available at the day-ahead stage for each dispatch model.

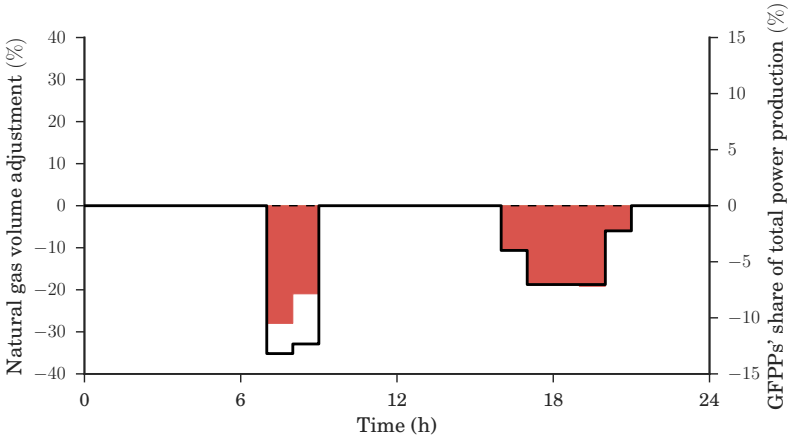

FIGURE 9. Hourly natural gas volume adjustment (black line: left y-axis) and difference in GFPPs' share of total power production between *V-B* and *Seq* (colored areas: right y-axis). Wind power penetration 50%. (Figure from [5])

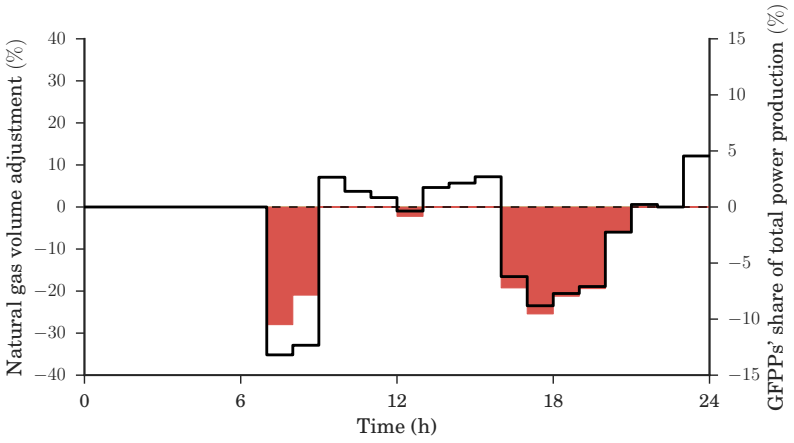

FIGURE 10. Hourly natural gas volume adjustment (black line: left y-axis) and difference in GFPPs' share of total power production between *V-B gen* and *Seq* (colored areas: right y-axis). Wind power penetration 50%. (Figure from [5])

It can be noticed in Figure 9 that a decrease in the natural gas volume results in a decrease of the power production share of GFPPs compared to the scheduling provided from model *Seq*. A similar effect is also observed in Figure 10, except for two periods in the middle of the day. During these hours, the total natural gas consumed by GFFPs in *V-B gen* is higher than in *Seq*, while GFPPs' share of total power production is not affected. This happens because there is a sift of "X MW" between the two GFPPs, resulting in the one with the higher power conversion factor to produce more than in *Seq*; hence increase the total gas consumption for power production.

Table 1 illustrates the performance of the dispatch models in terms of expected cost when the electricity demand is equal to 344 MW in order to explore an alternative case of natural gas price adjustment and volume availability. Models *Stoch* and *Seq* provide the two extreme solutions in terms of expected cost. We highlight though that *P-B*, *V-B* and *V-B gen* manage to return the same expected cost as *Stoch*. This fact illustrates that it is possible in specific cases to have an efficient sequential system dispatch if the future balancing costs are communicated into the day-ahead market through the operator-defined parameters χ.

TABLE 1. Expected system cost and its breakdown in $ when total power load is 344 MW

	Total	Day-ahead	Balancing	Up regulation	Down regulation
Seq	8,932.8	8,566.8	366.0	825.0	-459.0
Stoch	8,859.6	8,206.8	652.8	917.4	-264.6
P-B / V-B / V-B gen	8,859.6	8,638.8	220.8	679.8	-459.0

The schedule of power plants is given in Table 2 for D^{E}=344 MW. In *P-B*, the natural gas price adjustment is $\chi^{p}_{t_2}$ = +\$0.5/kcf which increases the marginal cost of GFPP I_4 to \$30/MWh. Thus, an improved day-ahead schedule is achieved by sifting 12 MW from GFPP I_4 to unit I_2, resulting in a lower expected cost. Models *V-B* and *V-B gen* reduce the total natural gas availability from 600 kcf to 456 kcf and return the same improved dispatch as *P-B*.

TABLE 2. Power system schedule in MW when total power load is 344 MW (variation from *Seq* day-ahead (DA) schedule in bold)

	Seq			*P-B*			*V-B*			*V-B gen*			*Stoch*		
Unit	DA	ω_1	ω_2	DA	ω_1	ω_2	DA	ω_1	ω_2	DA	ω_1	ω_2	DA	ω_1	ω_2
I_1	110	0	0	110	0	0	110	0	0	110	0	0	110	0	0
I_2	58	-10	+10	**70**	-10	+10	**70**	-10	+10	**70**	-10	+10	70	-10	+10
I_3	0	0	+5	0	0	0	0	0	0	0	0	0	0	0	0
I_4	50	-30	0	**38**	-30	+12	**38**	-30	+12	**38**	-30	+12	20	-12	+30
I_5	0	0	+25	0	0	+18	0	0	+18	0	0	+18	0	0	+18
WP	126	+40	-40	126	+40	-40	126	+40	-40	126	+40	-40	144	+22	-58

References

[1] J. Fortuny-Amat and B. McCarl, "A representation and economic interpretation of a two-level programming problem," *The Journal of the Operational Research Society*, vol. 32, no. 9, pp. 783–792, 1981.

[2] C. Ordoudis, *Market-based Approaches for the Coordinated Operation of Electricity and Natural Gas Systems*. PhD thesis, Technical University of Denmark, 2018.

[3] J. M. Morales, M. Zugno, S. Pineda, and P. Pinson, "Electricity market clearing with improved scheduling of stochastic production," *Eur. J. Oper. Res.*, vol. 235, pp. 765–774, Jun. 2014.

[4] A. Schwele, C. Ordoudis, J. Kazempour, and P. Pinson, "Coordination of power and natural gas systems: Convexification approaches for linepack modeling," in *2019 IEEE Milan PowerTech*, pp. 1–6, June 2019.

[5] C. Ordoudis, S. Delikaraoglou, P. Pinson, and J. Kazempour, "Exploiting flexibility in coupled electricity and natural gas markets: A price-based approach," in *2017 IEEE Manchester PowerTech*, pp. 1–6, June 2017.